

“Experimental measurement of carbohydrate-aromatic stacking in water by using a dangling-ended DNA model system”. Morales, J.C., Reina, J.J., Díaz, I., Aviñó, A., Nieto, P.M., Eritja, R. Chemistry Eur. J., 14(26), 7828-7835 (2008). doi: 10.1002/chem.200800335

**Experimental measurement of carbohydrate-aromatic stacking in water by using a
dangling-ended DNA model system**

Juan C. Morales^{a*}, José J. Reina^a, Irene Díaz^a, Anna Aviñó^b, Pedro Nieto^a, Ramón Eritja^b

^a Instituto de Investigaciones Químicas, CSIC – Universidad de Sevilla, 49 Americo Vesputio, 41092 Sevilla, Spain

^b Institute for Research in Biomedicine, Barcelona Science Park, IBMB – CSIC, CIBER – BBN Networking Centre on Bioengineering, Biomaterials and Nanomedicine, Josep Samitier 1, E-08028 Barcelona, Spain

*Corresponding author: (telephone 34-954-489-561; fax 34-954-460-565; e-mail: jcmorales@iiq.csic.es).

Abstract: Protein–carbohydrate recognition is of fundamental importance for a large number of biological processes; carbohydrate–aromatic stacking is a widespread, but poorly understood, structural motif in this recognition. We describe, for the first time, the measurement of carbohydrate–aromatic interactions from their contribution to the stability of a dangling-ended DNA model system. We observe clear differences in the energetics of the interactions of several monosaccharides with a benzene moiety depending on the number of hydroxy groups, the stereochemistry, and the presence of a methyl group in the pyranose ring. A fucose–benzene pair is the most stabilizing of the studied series (-0.4 Kcal mol⁻¹) and this interaction can be placed in the same range as other more studied interactions with aromatic residues of proteins, such as Phe–Phe, Phe–Met, or Phe–His. The noncovalent forces involved seem to be dispersion forces and nonconventional hydrogen bonds, whereas hydrophobic effects do not seem to drive the interaction.

Keywords: carbohydrate–aromatic stacking; carbohydrates; DNA; molecular recognition; stacking interactions

INTRODUCTION

Protein–carbohydrate interactions play a fundamental role within the living organisms in processes such as apoptosis, infection, inflammation, or fertilization.[1] Among the most cited noncovalent forces that participate in carbohydrate–protein recognition are hydrogen-bonding and ionic interactions. The role of water has also been mentioned to be a determinant driving force in this process.[2] In addition, a widespread, but poorly

understood, structural motif found between carbohydrates and proteins is the stacking of apolar patches of oligosaccharides with aromatic residues,[3] in which different noncovalent forces have been suggested to play a role, namely, CH- π interactions, Van der Waals forces, and hydrophobic effects.[4] Studies into carbohydrate-aromatic stacking interactions have been approached by using molecular biology tools,[5] NMR spectroscopy,[3b, 6] IR spectroscopy,[7] computational methods,[4a-c, 8] and model systems.[9] Artificial receptors that incorporate aromatics in their structure and take advantage of stacking interactions for carbohydrate recognition in apolar solvents have been reported.[10] Recently, a receptor containing *meta*-terphenyl units has been shown to bind cellobiose derivatives selectively in water.[11]

Nevertheless, few experimental binding data on sugar-arene stacking interactions have been reported and the quantification of these interactions has been attempted only in two specific examples. The interaction of a glucose-tyrosine pair as a transition-state stabilization was measured to be 0.7 kcalmol^{-1} in the -IV subsite of a 1,3-1,4- β -D-glucan-4-glucanohydrolase system, in which cooperativity could be playing a role.[12] Recently, a nonbiologically relevant tetraacetylglucose-tryptophan interaction was found to stabilize a hairpin-peptide model system by 0.8 kcalmol^{-1} . [13]

Herein, we describe the first model system in which carbohydrate-aromatic stacking interactions are measured and systematically studied. To do so, we quantified the contribution of two sugar-arene pairs to the stability of a dangling-ended DNA system. The energetic contributions of monosaccharide-benzene pairs in our DNA model system range from -0.15 to $-0.40 \text{ kcalmol}^{-1}$. The observed differences are due to the influence of the number of hydroxy groups, the stereochemistry, and the presence of a methyl group in the

pyranose ring. An upfield chemical shift of the NMR signals of all sugar protons in the oligonucleotide–carbohydrate conjugates confirmed the proximity of the carbohydrate to the face of the arene ring.

Results and Discussion

Design of the DNA model system: Our design of a dangling-ended DNA model is inspired by studies of aromatic stacking in DNA in which natural[14] or non-natural nucleosides[15] were placed at the end of a duplex in a “dangling” position. The resulting stabilization of the duplex was measured and compared with the duplex lacking the added nucleotides.

Our model system consists of a “dangling” benzene nucleoside with a covalently bound monosaccharide placed at the 5'-ends of a DNA duplex (Scheme 1A). The sugar is linked through an ethylene glycol spacer to a phosphate group located on the primary hydroxy group of the benzene nucleoside. This allows the pyranose ring to be on top of the benzene ring because it will be apart from the phosphate by the same distance as that found in a nucleoside between the base and its corresponding phosphate group (Scheme 1B). At the same time, this spacer allows enough freedom for the sugar to be either immersed in bulk water or in contact with the benzene ring. The DNA double helix acts as an energetic probe that allows the carbohydrate–aromatic interaction to be quantified when the carbohydrate–oligonucleotide conjugate is compared with the control lacking the carbohydrate moiety. In addition, the conjugate will allow the incorporation of different non-natural aromatic nucleosides and monosaccharides to quantify the interaction.

Synthesis of the carbohydrate–oligonucleotide conjugates: Preparation of the carbohydrate–oligonucleotide conjugates (COCs, **1–7**; Scheme 1C) was carried out by

standard solid-phase oligonucleotide automatic synthesis by using the DMT-phosphoramidite benzene nucleoside[16] and the corresponding carbohydrate phosphoramidite (DMT: 4,4'-di-methoxytriphenylmethyl). β -D-Glucose, β -D-2-deoxyglucose, α -D-2-deoxyglucose, β -D-galactose, and β -L-fucose were the monosaccharides selected to study how the interaction with a benzene ring is affected by different factors, such as the number of hydroxy groups, the anomeric configuration, the stereochemistry of the pyranose ring, and the presence of a methyl group.

The synthesis of the carbohydrate phosphoramidites was carried out in two steps. First, in the case of glucose, galactose, and fucose, attachment of the ethylene glycol spacer to the carbohydrate was carried out by classical glycosidation chemistry with the peracetylated bromo monosaccharides to obtain only the corresponding β isomers (Scheme 2). 2-Hydroxyethyl- 2,3,4,6-tetra-*O*-acetyl- β -D-glucopyranoside (**14**) and 2-hydroxyethyl-2,3,4,6-tetra-*O*-acetyl- β -D-galactopyranoside (**17**) were prepared as described previously,[17] and 2-hydroxyethyl-2,3,4-tri-*O*-acetyl- β -L-fucopyranoside (**20**) was synthesized following the same methodology. The 2-deoxyglucose derivatives were prepared by electrophilic addition to the corresponding acetyl-protected glucal and subsequent separation of the a and b isomers by column chromatography.[18] The corresponding carbohydrate phosphoramidites were then prepared by standard phosphoramidite chemistry (Scheme 2).[19]

Finally, the monosaccharide controls (**8–12**, Scheme 1C), used for structural comparison with the carbohydrate–oligonucleotide conjugates, were prepared in high yield by deprotection of the corresponding acetylated derivatives (**14**, **17**, **20**, **23**, and **24**) by classical methanolysis.

Thermodynamic parameters of the carbohydrate–DNA model systems: The measured thermodynamic parameters for the carbohydrate–oligonucleotide conjugates under physiological conditions (140 mM NaCl, 20 mM KCl, 10 mM phosphate buffer, pH 7) are illustrated in Table 1. The thermodynamic parameters were calculated from the average values obtained from melting curve fitting and linear plots of $1/T_m$ versus $\ln[\text{conjugate}]$.^[20] Calculation of the contribution of the carbohydrate–aromatic interaction to DNA stabilization was carried out by comparison of the corresponding carbohydrate–DNA conjugate with the control that lacks the pyranose ring but still maintains the ethylene glycol spacer (second row in Table 1). In fact, the presence of the linker destabilizes the DNA conjugate, most probably due to the entropy cost because of its high mobility, and this factor must be taken into account.

The thermodynamic data show that all of the conjugates that contain a carbohydrate–aromatic moiety show higher stability than the control conjugate **2**, most probably due to the affinity of the monosaccharides to stack with the benzene ring. It is important to note that the interaction is enthalpy driven, which seems to indicate the minor significance of classical hydrophobic effects in the interaction. Actually, the glucose–benzene interaction showed a stabilization of $-0.25 \text{ kcal mol}^{-1}$ in our dangling-ended DNA system.

Next, we investigated the effect of the number of hydroxyl groups in the pyranose ring on the interaction. β -Glucose stacks more strongly on the benzene ring than β -2-deoxyglucose, a more hydrophobic sugar that lacks the hydroxyl group at the 2-position. This result seems to support the fact that dispersion forces and nonconventional hydrogen bonds are the main noncovalent forces involved in this interaction, because the proton at the 2-position may be less polarized in β -2-deoxyglucose and, therefore, the interaction may lose one of the

nonconventional hydrogen bonds.[4a] When 2-deoxyglucose is attached in the α -anomeric configuration, the stacking is similar to that found for β -2-deoxyglucose. This result could indicate a similar stacking geometry with the aromatic moiety due to the high flexibility of the spacer, but the different chemical shifts of the NMR signals of the sugar protons seem to point to different approaches to the benzene ring (see the structural features section below).

The effect of the stereochemistry of the carbohydrate on the interaction was examined by comparison of β -glucose and β -galactose in their interactions with benzene. Surprisingly, the results show that stacking is stronger for glucose than for galactose, although a more extended apolar area in galactose could lead to the opposite result being predicted, especially if dispersion forces are involved in the interaction. A possible reason for this result could be that the ethylene glycol spacer is not long enough to allow the galactose moiety to adopt a more apical geometry and interact with the arene ring through the apolar patch formed by its H3–5 protons. Actually, the chemical-induced shifts of the NMR signals for the protons, obtained by comparing the sugar unit in conjugate **4** with the β -galactose control **9**, indicate a higher population of parallel-stacking geometry between the carbohydrate and the aromatic ring (see the structural features section below). In addition, it should be pointed out that the monosaccharides can approach the benzene unit through both faces of the pyranose ring due to the high flexibility of the linker. A stacking interaction with a parallel geometry between the β face of galactose and the aromatic ring is not possible due to the axial configuration of the hydroxyl group in the 4-position and, consequently, the potential contribution to the stability due to contacts through that face is lost in galactose but not in glucose (Figure 1).

It is important to note that the energetic data obtained refer to differences in stability between carbohydrate–DNA conjugates but these energetic values are an average of the different conformations available for each carbohydrate–DNA conjugate. Furthermore, the possibility of formation of a hydrogen bond between the 4-OH group of glucose and the arene moiety cannot be ruled out; this interaction is not possible in galactose without disrupting the parallel stacking with benzene, due to its intrinsic geometry. Similar reasoning should also be considered when comparing β -glucose and β -2-deoxyglucose. Actually, an H-bond between a glucose 4-OH group and toluene has been observed in the gas phase by IR spectroscopy,[7] and similar H-bonds have been observed in the X-ray crystal structures of proteins, such as between the hydroxy group of Thr13 and the center of the arene ring of Tyr6 in a class μ glutathione transferase.[21]

Finally, we studied the relevance of a methyl group in the structure of the pyranose ring. The contribution to DNA stabilization of the fucose–benzene interaction is $-0.40 \text{ kcal mol}^{-1}$, which makes this pair the most stable of the series. This carbohydrate–aromatic interaction is in the same range as other more studied interactions with aromatic residues of proteins, such as Phe–Phe, Phe–Met, or Phe–His.[22] The presence of the methyl group considerably increases the apolar surface of the carbohydrate and, therefore, dispersion forces involved in the interaction may be favored.

Structural features of the carbohydrate–aromatic stacking: ^1D and ^2D NMR experiments were carried out to study the geometry of the dangling moiety of the carbohydrate–oligonucleotide conjugates. We compared the chemical shifts of the resonances of the sugar protons in the carbohydrate–oligonucleotide conjugates (**3–7**) with those of the corresponding monosaccharide controls (**8–12**) that possess the linker moiety

but not the benzene nucleoside or the DNA strand. The comparison of the chemical shifts of the DNA resonances along the series of carbohydrate–oligonucleotide conjugates indicates no structural changes in the nucleic acid fragment. We observed that all of the proton resonances of the pyranose ring in the carbohydrate–oligonucleotide conjugates exhibited upfield shifting relative to those of the corresponding carbohydrate controls (Table 2). Comparison of the ^1H NMR spectrum of carbohydrate conjugate **5**, which contains the β -L-fucose unit, with that of the β -L-fucose control **10** clearly shows the upfield shift observed for all of the protons in the carbohydrate moiety (Figure 2). These data seem to confirm that all of the monosaccharides in the study prefer to stay close to the arene ring rather than just being immersed in the bulk water molecules. The proximity of the monosaccharides to the face of the arene ring could explain the extra stability found in the carbohydrate–oligonucleotide conjugates due to the presence of a potential carbohydrate–aromatic stacking interaction.

Moreover, the monosaccharides can approach the benzene unit through both faces of the pyranose ring, probably due to the high flexibility of the linker. It is important to note that the chemical-induced shifts show a similar trend in the four sugars linked to the DNA conjugate through a β -anomeric configuration. Upfield shift is more significant on the α face of the pyranose moiety, where protons H1, H3, and H5 are pointing down, as can be observed, for example, in β -glucose (Figure 3). This seems to indicate a more favourable interaction of the β -linked monosaccharides with the benzene ring through their α face. Actually, a similar geometric tendency has been found by Waters and co-workers between β -glucose and tryptophan in a β -hairpin-peptide model.[13]

In contrast to the results for sugars linked through a β -anomeric configuration to the DNA conjugate, the chemical-induced shifts for α -2-deoxyglucose show similar magnitude on both sides of the pyranose moiety. This could suggest that this sugar approaches the arene ring in a different way to the β -2-deoxyglucose and, therefore, different conformations are present during stacking with the aromatic moiety.

Finally, the β -2-deoxyglucose unit shows the largest resonance shifts of the series, even larger than those for β -L-fucose. This result is surprising since the stability measured is higher for β -L-fucose than for β -2-deoxyglucose during the interaction with benzene. This point to the fact that closer contact of β -2-deoxyglucose with the benzene ring may be possible due to the lack of a hydroxy group at the 2- position but this does not translate into a more favourable interaction.

Conclusion

Our results indicate that a dangling-ended DNA model system is a useful tool to measure carbohydrate–aromatic stacking interactions. Clear differences have been observed in the energetics of the interaction depending on the number of hydroxy groups, the stereochemistry, and the presence of a methyl group in the pyranose ring. The noncovalent forces involved seem to be dispersion forces and nonconventional hydrogen bonds between the protons of the pyranose ring and the benzene ring, whereas classical hydrophobic effects do not seem to drive the interaction. Investigations into the influence of other aromatic rings in the interaction and NMR spectroscopy and molecular modelling studies are in progress to obtain a better understanding of carbohydrate–aromatic stacking interactions by using our dangling-ended DNA model system.

Experimental Section

General remarks: All chemicals were obtained from Aldrich Chemicals and used without further purification, unless otherwise noted. All reactions were monitored by TLC on precoated silica gel 60 F₂₅₄ plates (Merck), with detection by heating with Mostain (10% H₂SO₄ (500 mL), (NH₄)₆Mo₇O₂₄·4H₂O (25 g), Ce(SO₄)₂·4H₂O (1 g)). Products were purified by flash chromatography with Merck silica gel 60 (200–400 mesh). High-resolution FAB (+) mass spectral analyses were obtained on a Micromass AutoSpec-Q spectrometer.

NMR spectra were recorded on Bruker AVANCE 300, ARX 400, or Avance DRX 500 MHz spectrometers (300 or 400 MHz (¹H), 75 or 100 (¹³C); 500 MHz for the carbohydrate controls and for the carbohydrate–DNA conjugate samples) at room temperature for solutions in CDCl₃, D₂O, or CD₃OD. Chemical shifts were referenced to the solvent signal. 2D experiments (COSY, TOCSY, ROESY, and HMQC) were done when necessary to assign resonances of the oligosaccharides or the carbohydrate–DNA conjugates. The carbohydrate–DNA samples for NMR spectroscopy were purified by HPLC and then ion-exchanged with Dowex 50W resin. Finally, samples were lyophilized to dryness three times from D₂O to deuterate all exchangeable protons and dissolved in 99.999% D₂O just prior to recording of the NMR spectra. Sample concentration ranged from 0.7 to 2.8 mM depending on the conjugate. Chemical shifts (δ) are given in ppm with respect to the acetone signal, which was used as an external reference (volume of 1 μL). In all experiments, the ¹H carrier frequency was kept at the water resonance. Data were processed by using the

manufacturer software, raw data were multiplied by a shifted exponential window function prior to Fourier transformation, and the baseline was corrected by using polynomial fitting. Melting curves for the DNA conjugates were measured in a Perkin–Elmer Lambda 12 UV/Vis spectrophotometer at 280 nm while the temperature was raised from 20 to 80°C at a rate of 1.0 °C min⁻¹. Curve fits were excellent, with χ^2 values of 10⁻⁶ or better, and the Van't Hoff linear fits were quite good ($r^2=0.98$) for all oligonucleotides. Differences of less than 10% were observed between thermodynamic parameters as determined by $1/T_m$ versus $\ln[\text{conjugate}]$ plots and curve fittings. ΔH , ΔS , and ΔG errors were calculated as described previously.[20]

Preparation of carbohydrate alcohols and phosphoramidites.

2-Hydroxyethyl-2,3,4-tri-*O*-acetyl- β -l-fucopyranoside (20): Na₂SO₄ (7 spatula tips) and ethylene glycol (2.0 mL, 35.86 mmol, 18 equiv) were added to a solution of tri-*O*-acetylfucopyranosyl bromide (0.68 g, 1.93 mmol) in anhydrous CH₂Cl₂ (40 mL). After the mixture had been stirred at room temperature for 15 min under an argon atmosphere, Ag₂CO₃ (9.00 g, 16.31 mmol, 8.5 equiv) was added to the reaction mixture and stirring was continued for 18 h (TLC: hexane (Hex)/EtOAc 2:3). The mixture was filtered, diluted with CH₂Cl₂ (40 mL), washed with water (3x100 mL), and dried over anhydrous MgSO₄; the solvent was then evaporated under reduced pressure. The product was purified by silica gel column chromatography by using Hex/EtOAc (2:3) as the eluent to give compound 20 (0.4 g, 62%) as a syrup. ¹H NMR (300 MHz, CDCl₃): δ =5.19 (dd, ³*J*(H,H)=0.5, 3.0 Hz, 1H; H4), 5.14 (dd, ³*J*(H,H)=7.8, 10.5 Hz, 1H; H2), 4.98 (dd, ³*J*(H,H)=3.3, 10.5 Hz, 1H; H3), 4.44 (d, ³*J*(H,H)=7.8 Hz, 1H; H1), 3.84–3.66 (m, 5H; H5, 2xH7, 2xH8), 2.64 (br s, 1H;

OH), 2.14, 2.04, 1.94 (3 s, 9H; 3xOCOCH₃), 1.19 ppm (d, ³J(H,H)=6.3 Hz, 3H; CH₃); ¹³C NMR (75 MHz, CDCl₃): δ=170.4, 169.9, 169.6, 101.2, 71.9, 70.9, 69.9, 68.9, 68.7, 61.4, 20.5, 20.4, 20.3, 15.7 ppm; FAB HRMS: m/z: calcd for C₁₄H₂₂O₉: 334.1264 [M]⁺; found: 357.1167 [M+Na]⁺.

2-Hydroxyethyl-3,4,6-tri-O-acetyl-2-deoxy-α,β-D-glucopyranoside (23, 24): A solution of PPh₃·HBr (0.71 g, 2.07 mmol) and ethylene glycol in dry CH₂Cl₂ (25 mL) was added to a solution of tri-O-acetyl-glucal (7.5 g, 27.5 mmol) in dry CH₂Cl₂ (8 mL). The reaction mixture was stirred at 40°C. After 24 h, more PPh₃·HBr (2.13 g, 6.21 mmol) was added to the reaction mixture, and stirring was continued for 7 h. The reaction was then stopped by addition of CH₂Cl₂ (120 mL) and water (150 mL). The organic phase was washed with saturated NaHCO₃ (3x150 mL), dried over anhydrous Na₂SO₄, and filtered; the solvent was then evaporated to dryness. The final product was purified by silica gel column chromatography by using a solvent gradient (Hex/EtOAc 5:4, 1:1, 4:5, 2:3) to obtain β isomer **23** (460 mg, 5%), α isomer **24** (1.84 g, 20%), and a fraction mixture of **23** and **24** (1.38 g, 15%). ¹H NMR (300 MHz, CDCl₃): β isomer **23**: δ=5.03–4.86 (m, 2H; H3, H4), 4.58 (d, ³J(H,H)=9.6 Hz, 1H; H1), 4.18 (dd, ³J(H,H)=5.6, ²J(H,H)=12.2 Hz, 1H; H6a), 4.12 (t, ²J(H,H)=11.7 Hz, 1H; H6b), 3.82–3.59 (m, 5H; H5, 2xH7, 2xH8), 2.74 (t, ³J(H,H)=6.1 Hz, 1H; OH), 2.32 (dd, ³J(H,H)=4.7, ²J(H,H)=12.5 Hz, 1H; H2_{eq}), 2.05, 2.00, 1.99 (3 s, 9H; 3xOCOCH₃), 1.72 ppm (q, ²J(H,H)=11.0 Hz, 1H; H2_{ax}); ¹³C NMR (75 MHz, CDCl₃): β isomer **23**: δ=170.6, 170.2, 169.7, 100.1, 72.7, 71.9, 70.3, 68.9, 62.4, 62.0, 36.0, 20.8, 20.6 ppm; FAB HRMS: β isomer **23**: m/z: calcd for C₁₄H₂₂O₉: 334.1264 [M]⁺; found: 357.1165 [M+Na]⁺. ¹H NMR (300 MHz, CDCl₃): α isomer **24**: δ=5.25 (ddd, ³J(H,H)=5.3, 9.5, 11.5 Hz, 1H; H3) 4.96–4.89 (m, 2H; H1, H4), 4.94 (dd, ³J(H,H)=4.5, ²J(H,H)=12.4 Hz, 1H;

H6a), 4.00 (dd, $^3J(\text{H,H})=2.2$, $^2J(\text{H,H})=12.3$ Hz, 1H; H6b), 4.01–3.92 (m, 1H; H5), 3.70–3.64 (m, 3H; H7a, 2xH8), 3.54–3.47 (m, 1H; H7b), 2.7 (br s, 1H; OH), 2.22 (dd, $^3J(\text{H,H})=5.3$, $^2J(\text{H,H})=12.9$ Hz, 1H; H_{2eq}), 2.02, 1.97, 1.95 (3 s, 9H; 3xOCOCH₃), 1.77 ppm (dt, 1H, $^3J(\text{H,H})=3.6$, $^2J(\text{H,H})=12.9$ Hz; H_{2ax}); ¹³C NMR (75 MHz, CDCl₃): α isomer **24**: δ=170.4, 170.0, 169.6, 96.9, 69.1, 69.0, 68.7, 67.6, 62.0, 61.1, 34.6, 20.6, 20.4, 20.3 ppm; FAB HRMS: m/z: a isomer **24**: calcd for C₁₄H₂₂O₉ : 334.1264 [M]⁺; found: 357.1167 [M+Na]⁺.

β-Cyanoethoxy-β-(2,3,4,6-tetra-O-acetyl-β-D-glucopyranosyl)ethoxy-diisopropylamine phosphine (15): DIEA (0.49 mL, 3.72 mmol) and 2-cyanoethyl-*N,N'*-diisopropylamino-chlorophosphoramidite (170 μL, 0.76 mmol) were added to a solution of 2-hydroxyethyl-2,3,4,6-tetra-*O*-acetyl-β-D-glucopyranoside (**14**;[17] 0.2 g, 0.51 mmol) in anhydrous CH₂Cl₂ (4 mL) at room temperature under an argon atmosphere. After 1.5 h, the solution was diluted with EtOAc (20 mL), and the organic phase was washed with brine (3x25 mL), dried over anhydrous MgSO₄, and filtered; the solvent was then evaporated to dryness. The product was purified by silica gel column chromatography by using Hex/EtOAc (2:1 with 2% of NEt₃) as the eluent to give compound **15** (215 mg, 74%) as a syrup. ¹H NMR (300 MHz, CDCl₃): mixture of isomers: δ=5.11 (t, $^3J(\text{H,H})=9.4$ Hz, 1H; H3), 4.99 (t, $^3J(\text{H,H})=9.6$ Hz, 1H; H4), 4.89 (t, $^3J(\text{H,H})=8.0$ Hz, 1H; H2), 4.55 (t, $^3J(\text{H,H})=8.6$ Hz, 1H; H1), 4.18 (dd, $^3J(\text{H,H})=2.6$, $^2J(\text{H,H})=12.1$ Hz, 1H; H6a), 4.06–3.99 (m, 1H; H6b), 3.89–3.45 (m, 9H; H5, 2xH7, 2xH8, OCH₂CH₂CN, 2xCHisopropyl), 2.56 (m, 2H; OCH₂CH₂CN), 1.99, 1.97, 1.96, 1.93, 1.91 (5 s, 12H; 4xOCOCH₃), 1.09 ppm (2 d, $^3J(\text{H,H})=6.2$ Hz, 12H; 4xCH₃isopropyl); ¹³C NMR (75 MHz, CDCl₃): mixture of isomers: δ=170.4, 170.0, 169.2, 169.1, 169.1, 117.6, 100.6, 72.6, 72.6, 72.5, 71.5, 71.0, 69.4, 69.3,

69.2, 69.1, 68.1, 68.1, 62.4, 62.3, 62.2, 62.1, 61.7, 60.1, 58.4, 58.3, 58.1, 58.0, 42.9, 42.9, 42.8, 42.7, 24.4, 24.4, 24.3, 24.3, 20.8, 20.5, 20.4, 20.2, 20.2, 20.1, 20.1 ppm; FAB HRMS: m/z: calcd for C₂₅H₄₁N₂O₁₂P: 592.2397 [M]⁺; found: 615.2294 [M+Na]⁺.

β-Cyanoethoxy-β-(2,3,4,6-tetra-O-acetyl-β-D-galactopyranosyl)ethoxy-diisopropylamine phosphine (18): DIEA (0.96 mL, 3.72 mmol) and 2-cyanoethyl- *N,N'*-diisopropylamino-chlorophosphoramidite (332 μL, 1.49 mmol) were added to a solution of 2-hydroxyethyl-2,3,4,6-tetra-*O*-acetyl-β-D-galactopyranoside (**17**;[17] 0.39 g, 0.99 mmol) in dry CH₂Cl₂ (4 mL) at room temperature under an argon atmosphere. After 1.5 h, the solution was diluted with EtOAc (20 mL), and the organic phase was washed with brine (3x25 mL), dried over anhydrous MgSO₄, and filtered; the solvent was then evaporated to dryness. The product was purified by silica gel column chromatography by using Hex/EtOAc (2:3 with 2% of NEt₃) as the eluent to give compound **18** (368 mg, 84%) as a syrup. ¹H NMR (300 MHz, CDCl₃): mixture of isomers: δ=5.32 (d, ³*J*(H,H)=2.9 Hz, 1H; H4), 5.13 (ddd, ³*J*(H,H)=2.2, 8.0, 10.3 Hz, 1H; H2), 4.95 (dt, ³*J*(H,H)=3.6, 10.3 Hz, 1H; H3), 4.53 (t, ³*J*(H,H)=7.5 Hz, 1H; H1), 4.15–4.01 (m, 2H; 2xH6), 3.95–3.45 (m, 9H; H5, 2xH7, 2xH8, OCH₂CH₂CN, 2xCHisopropyl), 2.59 (t, ³*J*(H,H)=6.1 Hz, 2H; OCH₂CH₂CN), 2.09, 2.01, 2.00, 1.94, 1.91 (5 s, 12H; 4xOCOCH₃), 1.12 ppm (2 d, ³*J*(H,H)=6.5 Hz, 12H; 4xCH₃isopropyl); ¹³C NMR (75 MHz, CDCl₃): mixture of isomers: δ=170.2, 170.1, 170.0, 169.3, 117.6, 101.1, 101.0, 70.7, 70.4, 69.4, 69.3, 69.1, 69.0, 68.6, 68.5, 66.9, 66.8, 62.4, 62.3, 62.2, 62.1, 61.1, 61.0, 58.4, 58.3, 58.1, 58.1, 43.0, 42.9, 42.8, 24.5, 24.4, 24.4, 24.3, 20.7, 20.5, 20.5, 20.4, 20.3, 20.3, 20.2, 20.2 ppm; FAB HRMS: m/z: calcd for C₂₅H₄₁N₂O₁₂P: 592.2397 [M]⁺; found: 592.2397 [M+Na]⁺.

β -Cyanoethoxy- β -(2,3,4,-tri-*O*-acetyl- β -L-fucopyranosyl)ethoxy-diisopropylamine

phosphine (21): DIEA (0.51 mL, 2.92 mmol) and 2-cyanoethyl- *N,N'*-diisopropylamino-chlorophosphoramidite (260 μ L, 1.18 mmol) were added to a solution of 2-hydroxyethyl-2,3,4-tri-*O*-acetyl- β -L-fucopyranoside (**20**; 0.26 g, 0.78 mmol) in dry CH_2Cl_2 (4 mL) at room temperature under an argon atmosphere. After 1.5 h, the solution was diluted with EtOAc (20 mL), and the organic phase was washed with brine (3x25 mL), dried over anhydrous MgSO_4 , and filtered; the solvent was then evaporated to dryness. The product was purified by silica gel column chromatography by using Hex/EtOAc (2:1 with 2% NEt_3) as the eluent to give compound **21** as a syrup (200 mg, 48%). ^1H NMR (300 MHz, CDCl_3): mixture of isomers: δ =5.18 (d, $^3J(\text{H,H})$ =3.3 Hz, 1H; H4), 5.13 (ddd, $^3J(\text{H,H})$ =2.4, 7.9, 10.4 Hz, 1H; H2), 4.96 (dt, $^3J(\text{H,H})$ =3.8, 10.4 Hz, 1H; H3), 4.51 (m, $^3J(\text{H,H})$ =8.3 Hz, 1H; H1), 3.98–3.48 (m, 9H; H5, 2xH7, 2xH8, $\text{OCH}_2\text{CH}_2\text{CN}$, 2xCHisopropyl), 2.60 (t, $^3J(\text{H,H})$ =6.3 Hz, 1H; $\text{OCH}_2\text{CH}_2\text{CN}$), 2.13, 2.03, 2.02, 1.93 (4 s, 9H; 3x OCOCH_3), 1.18 (d, $^3J(\text{H,H})$ =6.3, 3H; CH_3), 1.14 ppm (2 d, $^3J(\text{H,H})$ =6.7 Hz, 12H; 4x CH_3 isopropyl); ^{13}C NMR (75 MHz, CDCl_3): mixture of isomers: δ =170.6, 170.1, 169.4, 117.7, 101.0, 100.9, 71.2, 71.2, 70.2, 70.1, 69.3, 69.2, 69.0, 69.0, 68.9, 68.8, 68.7, 62.5, 62.4, 62.3, 62.2, 58.5, 58.2, 43.0, 43.0, 42.9, 42.8, 24.5, 24.5, 24.4, 20.8, 20.8, 20.6, 20.5, 20.3, 20.3, 15.9 ppm; FAB HRMS: m/z: calcd for $\text{C}_{23}\text{H}_{41}\text{N}_2\text{O}_{10}\text{P}$: 534.2342 $[\text{M}]^+$; found: 557.2240 $[\text{M}+\text{Na}]^+$.

β -Cyanoethoxy- β -(3,4,6-tri-*O*-acetyl-2-deoxy- β -D-glucopyranosyl)ethoxydiisopropyl-

amine phosphine (25): DIEA (0.39 mL, 2.24 mmol) and 2-cyanoethyl-*N,N'*-diisopropylamino-chlorophosphoramidite (200 μ L, 0.9 mmol) were added to a solution of 2-hydroxyethyl-2,3,4-tri-*O*-acetyl-2-deoxy- β -D-glucopyranoside (**23**; 0.2 g, 0.6 mmol) in anhydrous CH_2Cl_2 (4 mL) at room temperature under an argon atmosphere. After 1.5 h, the

solution was diluted with EtOAc (20 mL), and the organic phase was washed with brine (3x25 mL), dried over anhydrous MgSO₄, and filtered; the solvent was then evaporated to dryness. The product was purified by silica gel column chromatography by using Hex/EtOAc (2:1 with 2% of NEt₃) as the eluent to give compound **25** (284 mg, 89%) as a syrup. ¹H NMR (300 MHz, CDCl₃): mixture of isomers: δ=4.98–4.79 (m, 2H; H3, H4), 4.56 (d, ³J(H,H)=9.4 Hz, 1H; H1), 4.19 (dd, ³J(H,H)=4.4, ²J(H,H)=12.1 Hz, 1H; H6a), 4.06–3.92 (m, 1H; H6b), 3.92–3.40 (m, 9H; H5, 2xH7, 2xH8, OCH₂CH₂CN, 2xCHisopropyl), 2.56 (t, ³J(H,H)=6.2 Hz, 2H; OCH₂CH₂CN), 2.22 (dd, ³J(H,H)=4.4, ²J(H,H)=10.0 Hz, 1H; H2_{eq}), 1.97, 1.92, 1.91 (3 s, 9H; 3xOCOCH₃), 1.71–1.53 ppm (m, 1H; H2_{ax}); ¹³C NMR (75 MHz, CDCl₃): mixture of isomers: δ=170.4, 170.0, 169.9, 169.5, 117.5, 99.5, 99.4, 71.6, 71.6, 70.3, 69.1, 69.0, 68.8, 68.7, 62.4, 62.3, 62.1, 58.4, 58.3, 58.1, 42.9, 42.7, 35.9, 24.4, 24.4, 24.3, 20.7, 20.6, 20.5 ppm; FAB HRMS: m/z: calcd for C₂₅H₃₉N₂O₁₀P: 534.2342 [M]⁺; found: 557.2240 [M+Na]⁺.

β-Cyanoethoxy-β-(3,4,6-tri-O-acetyl-2-deoxy-α-D-glucopyranosyl)ethoxydiisopropyl-aminophosphine (26): DIEA (0.59 mL, 3.38 mmol) and 2-cyanoethyl-*N,N'*-diisopropylamino-chlorophosphoramidite (0.3 mL, 1.35 mmol) were added to a solution of 2-hydroxyethyl-2,3,4-tri-*O*-acetyl-2-deoxy-α-D-glucopyranoside (**24**; 0.3 g, 0.9 mmol) in dry CH₂Cl₂ (4 mL) at room temperature under an argon atmosphere. After 1 h, the solution was diluted with EtOAc (20 mL), and the organic phase was washed with brine (3x25 mL), dried over anhydrous MgSO₄, and filtered; the solvent was then evaporated to dryness. The product was purified by silica gel column chromatography by using Hex/EtOAc (3:2 with 2% of NEt₃) as the eluent to give compound **26** (410 mg, 85%) as a syrup. ¹H-NMR (300 MHz, CDCl₃): mixture of isomers: δ=5.33–5.36 (m, 1H; H3), 5.02–4.88 (m, 2H; H1, H4),

4.25 (dd, $^3J(\text{H,H})=4.4$, $^2J(\text{H,H})=12.3$ Hz, 1H; H6a), 4.08–3.91 (m, 2H; H5, H6b), 3.91–3.65 (m, 5H; H7a, 2xH8, OCH₂CH₂CN), 3.65–3.44 (m, 3H; H7b, 2xCHisopropyl), 2.63 (t, $^3J(\text{H,H})=6.2$ Hz, 2H; OCH₂CH₂CN), 2.20 (dd, $^3J(\text{H,H})=5.2$, $J(\text{H,H})=12.8$ Hz, 1H; H2eq), 2.04, 1.98, 1.95 (3 s, 9H; 3xOCOCH₃), 1.76 (dt, $^3J(\text{H,H})=3.0$, $^2J(\text{H,H})=12.2$ Hz, 1H; H2ax), 1.14 ppm (d, $^3J(\text{H,H})=6.7$ Hz, 12H; 4xCH₃isopropyl); ¹³C NMR (75 MHz, CDCl₃): mix of isomers: $\delta=170.7$, 170.7, 170.2, 169.9, 117.7, 97.1, 97.0, 69.3, 69.3, 69.1, 69.0, 67.9, 67.8, 67.6, 67.5, 67.4, 62.5, 62.4, 62.3, 62.2, 58.6, 58.4, 43.2, 43.1, 24.7, 24.6, 21.0, 20.8, 20.7, 20.4, 20.3 ppm; FAB HRMS: m/z: calcd for C₂₃H₃₉N₂O₁₀P: 534.2342 [M]⁺; found: 573.2120 [M+K]⁺.

1-Hydroxyethyl- β -D-glucopyranoside (8): NaOMe (27 mg, 0.50 mmol) was added to a solution of 2-hydroxyethyl-2,3,4,6-tetra-*O*-acetyl- β -D-glucopyranoside (**14**; 100 mg, 0.25 mmol) in MeOH (3 mL), and the reaction was stirred at room temperature for 30 min. The solution was then neutralized with Amberlite IRA-120 resin and filtered, and the solvent was eliminated in vacuo to obtain compound **8** (56 mg, quant yield) as a white solid. ¹H NMR (500 MHz, D₂O): $\delta=4.49$ (d, $^3J(\text{H,H})=7.9$ Hz, 1H; H1), 3.98 (m, 1H; H7a), 3.91 (dd, $^3J(\text{H,H})=2.2$, 12.3 Hz, 1H; H6b), 3.77 (m, 3H; H7b, 2TH8) 3.72 (dd, $^3J(\text{H,H})=6.0$, 12.3 Hz, 1H; H6a), 3.50 (t, $^3J(\text{H,H})=9.2$ Hz, 1H; H3), 3.45 (m, 1H; H5), 3.39 (t, $^3J(\text{H,H})=9.4$ Hz, 1H; H4), 3.31 ppm (dd, $^3J(\text{H,H})=8.0$, 9.4 Hz, 1H; H6b); ¹³C NMR (100 MHz, CD₃OD): $\delta=103.1$, 76.6, 76.5, 73.8, 71.0, 70.2, 61.3, 60.9 ppm; ESIMS: m/z: calcd for C₂₅H₄₁N₂O₁₂P: 592.2397 [M]⁺; found: 592.2397 [M+Na]⁺.

1-Hydroxyethyl- β -D-galactopyranoside (9): NaOMe (27 mg, 0.50 mmol) was added to a solution of 2-hydroxyethyl-2,3,4,6-tetra-*O*-acetyl- β -D-galactopyranoside (**17**; 100 mg, 0.25 mmol) in MeOH (3 mL), and the reaction was stirred at room temperature for 30 min. The

solution was then neutralized with Amberlite IRA-120 resin and filtered, and the solvent was eliminated *in vacuo* to obtain compound **9** (56 mg, quant yield) as a white solid. ^1H NMR (500 MHz, D_2O): δ =4.42 (d, $^3J(\text{H,H})=7.8$ Hz, 1H; H1), 4.05 (m, 1H; H7a), 3.92 (d, $^3J(\text{H,H})=3.4$ Hz, 1H; H4), 3.81–3.75 (m, 4H; H6a, H7b, 2xH8), 3.74 (dd, $^3J(\text{H,H})=4.2$, 11.7 Hz, 1H; H6b), 3.70 (dd, $^3J(\text{H,H})=4.2$, 8.0 Hz, 1H; H5), 3.65 (dd, $^3J(\text{H,H})=3.5$, 10.8 Hz, 1H; H3), 3.55 ppm (dd, $^3J(\text{H,H})=7.9$, 10.0 Hz, 1H; H2); ^{13}C -NMR (100 MHz, CD_3OD): δ =103.8, 75.3, 73.5, 71.3, 70.0, 68.9, 61.1, 61.0 ppm; ESIMS: m/z: calcd for $\text{C}_8\text{H}_{16}\text{O}_7$: 224.1 $[\text{M}]^+$; found: 247.1 $[\text{M}+\text{Na}]^+$.

1-Hydroxyethyl- β -l-fucopyranoside (10): NaOMe (32 mg, 0.60 mmol) was added to a solution of 2-hydroxyethyl-2,3,4-tri-*O*-acetyl- β -L-fucopyranoside (**20**; 100 mg, 0.30 mmol) in MeOH (3 mL), and the reaction was stirred at room temperature for 30 min. The solution was then neutralized with Amberlite IRA-120 resin and filtered, and the solvent was eliminated *in vacuo* to obtain compound **10** (53 mg, 86%) as a white solid. ^1H NMR (500 MHz, D_2O): δ =4.90 (d, $^3J(\text{H,H})=7.9$ Hz, 1H; H1), 3.98 (m, 1H; H7a), 3.90 (dd, $^3J(\text{H,H})=6.5$, 7.6 Hz, 1H; H7b) 3.77(m, 1H; H5), 3.76 (m, 2H; 2xH8) 3.74 (m, 1H; H4), 3.64 (dd, $^3J(\text{H,H})=3.5$, 10.0 Hz, 1H; H3), 3.50 (dd, $^3J(\text{H,H})=7.9$, 10.0 Hz, 1H; H2), 1.25 ppm (d, $^3J(\text{H,H})=6.5$ Hz, 1H; CH_3); ^{13}C NMR (100 MHz, CD_3OD): δ =103.6, 73.6, 71.6, 71.0, 70.8, 70.6, 61.0, 15.3 ppm; ESIMS: m/z: calcd for $\text{C}_8\text{H}_{16}\text{O}_7$: 208.1 $[\text{M}]^+$; found: 231.1 $[\text{M}+\text{Na}]^+$.

1-Hydroxyethyl-2-deoxy- β -D-glucopyranoside (11): NaOMe (16 mg, 0.30 mmol) was added to a solution of 2-hydroxyethyl-2,3,4-tri-*O*-acetyl-2-deoxy- β -D-glucopyranoside (**23**; 50 mg, 0.15 mmol) in MeOH (2 mL), and the reaction was stirred at room temperature for 30 min. The solution was then neutralized with Amberlite IRA-120 resin and filtered, and

the solvent was eliminated *in vacuo* to obtain compound **11** (31 mg, quant yield) as a white solid. ^1H NMR (500 MHz, D_2O): $\delta=4.74$ (dd, $^3J(\text{H,H})=1.5, 9.8$ Hz, 1H; H1), 3.96 (m, 1H; H7) 3.92 (dd, $^3J(\text{H,H})=2.3, 12.3$ Hz, 1H; H6b), 3.74 (m, 4H; H6a, H7b, 2xH8) 3.71 (dd, $^3J(\text{H,H})=1.5, 9.8$ Hz, 1H; H4), 3.38 (ddd, $^3J(\text{H,H})=2.0, 6.5, 9.0$ Hz, 1H; H5), 3.26 (t, $^3J(\text{H,H})=9.6$ Hz, 1H; H4), 2.29 (ddd, $^3J(\text{H,H})=1.8, 4.6, ^2J(\text{H,H})=12.1$ Hz, 1H; H2_{eq}), 1.52 ppm (dt, $^3J(\text{H,H})=10.6, ^2J(\text{H,H})=12.1$ Hz, 1H; H2_{ax}); ^{13}C NMR (100 MHz, CD_3OD): $\delta=100.0, 76.6, 71.7, 71.2, 70.5, 61.5, 61.0, 38.9$ ppm; ESIMS: m/z: calcd for $\text{C}_8\text{H}_{16}\text{O}_6$: 208.1 $[\text{M}]^+$; found: 231.1 $[\text{M}+\text{Na}]^+$.

1-Hydroxyethyl-2-deoxy- α -D-glucopyranoside (12): NaOMe (16 mg, 0.30 mmol) was added to a solution of 2-hydroxyethyl-2,3,4-tri-*O*-acetyl-2-deoxy- α -D-glucopyranoside (**24**; 50 mg, 0.15 mmol) in MeOH (2 mL), and the reaction was stirred at room temperature for 30 min. The solution was then neutralized with Amberlite IRA-120 resin and filtered, and the solvent was eliminated *in vacuo* to obtain compound **12** (31 mg, quant yield) as a white solid. ^1H NMR (500 MHz, D_2O): $\delta=4.74$ (dd, $^3J(\text{H,H})=1.5, 9.8$ Hz, 1H; H1), 3.96 (m, 1H; H7) 3.92 (dd, $^3J(\text{H,H})=2.3, 12.3$ Hz, 1H; H6b), 3.74 (m, 4H; H6a, H7b, 2TH8) 3.71 (dd, $^3J(\text{H,H})=1.5, 9.8$ Hz, 1H; H4), 3.38 (ddd, $^3J(\text{H,H})=2.0, 6.5, 9.0$ Hz, 1H; H5), 3.26 (t, $^3J(\text{H,H})=9.6$ Hz, 1H; H4), 2.29 (ddd, $^3J(\text{H,H})=1.8, 4.60, ^2J(\text{H,H})=12.1$ Hz, 1H; H2_{eq}), 1.52 ppm (dt, $^3J(\text{H,H})=10.6, ^3J(\text{H,H})=12.1$ Hz, 1H; H2_{ax}); ^{13}C NMR (100 MHz, CD_3OD): $\delta=100.0, 76.6, 71.7, 71.2, 70.5, 61.5, 61.0, 38.9$ ppm; ESIMS: m/z: calcd for $\text{C}_8\text{H}_{16}\text{O}_6$: 208.1 $[\text{M}]^+$; found: 231.1 $[\text{M}+\text{Na}]^+$.

Synthesis of carbohydrate-oligonucleotide conjugates 1-7: Carbohydrate-oligonucleotide conjugates were synthesized on an Applied Biosystems 394 synthesizer by using standard β -cyanoethylphosphoramidite chemistry. The benzene DMT-

phosphoramidite derivative was prepared as previously described.[16] Oligonucleotide conjugates were synthesized on a 0.2 or 1.0 μmol scale low-volume resin and in DMT-off mode. DMTethane phosphoramidite was purchased from Chemgenes Corp. Oligonucleotide supports were treated with 33% aqueous ammonia for 16 h at 55°C, then the ammonia solutions were evaporated to dryness and the conjugates were purified by reversed-phase HPLC in a Waters Alliance separation module with a PDA detector. HPLC conditions were as follows: Nucleosil 120 C18, 250x8 mm 10 μm column; flow rate: 3 mLmin^{-1} ; 27 min linear gradient 0-30%B (solvent A: 5% CH_3CN / 95% 100 mM triethylammonium acetate (TEAA; pH 6.5); solvent B: 70% CH_3CN /30% 100 mM TEAA (pH 6.5)).

Acknowledgements

We thank the Ministry of Science and Education for funding (grant no.: CTQ-2006-01123/BQU) and for a Ramón y Cajal contract (J.C.M.).

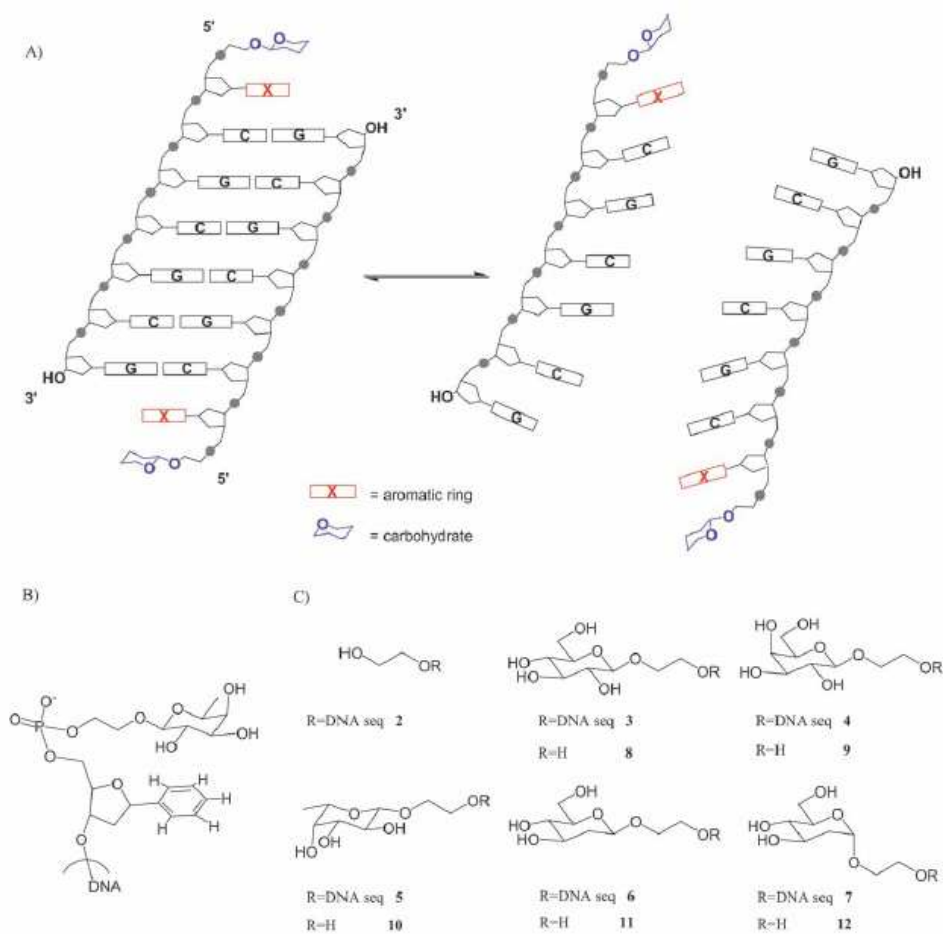
References

- [1] a) T. Feizi, *Adv. Exp. Med. Biol.* 1998, 435, 51; b) R. A. Dwek, *Chem. Rev.* 1996, 96, 683; c) A. Varki, *Glycobiology* 1993, 3, 97; d) H. J. Gabius, H. C. Siebert, S. Andre, J. Jimenez-Barbero, H. Rudiger, *ChemBioChem* 2004, 5, 740.
- [2] R. U. Lemieux, *Acc. Chem. Res.* 1996, 29, 373.
- [3] a) A. B. Boraston, D. N. Bolam, H. J. Gilbert, G. J. Davies, *Biochem. J.* 2004, 382, 769; b) H. Kogelberg, D. Solis, J. Jimenez-Barbero, *Curr. Opin. Struct. Biol.* 2003, 13, 646; c) H. Lis, N. Sharon, *Chem. Rev.* 1998, 98, 637.

- [4] a) M. C. Fernandez-Alonso, F. J. Canada, J. Jimenez-Barbero, G. Cuevas, *J. Am. Chem. Soc.* 2005, 127, 7379; b) M. S. Sujatha, Y. U. Sasidhar, P. V. Balaji, *Biochemistry* 2005, 44, 9554; c) V. Spiwok, P. Lipovova, T. Skalova, E. Buchtelova, J. Hasek, B. Kralova, *Carbohydr. Res.* 2004, 339, 2275; d) S. Elgavish, B. Shaanan, *Trends Biochem. Sci.* 1997, 22, 462; e) E. J. Toone, *Curr. Opin. Struct. Biol.* 1994, 4, 719.
- [5] a) J. Flint, D. Nurizzo, S. E. Harding, E. Longman, G. J. Davies, H. J. Gilbert, D. N. Bolam, *J. Mol. Biol.* 2004, 337, 417; b) L. Guan, Y. Hu, H. R. Kaback, *Biochemistry* 2003, 42, 1377; c) M. Kasahara, M. Maeda, *J. Biol. Chem.* 1998, 273, 29106; d) K. Maenaka, M. Matsushima, H. Song, F. Sunada, K. Watanabe, I. Kumagai, *J. Mol. Biol.* 1995, 247, 281.
- [6] G. Terraneo, D. Potenza, A. Canales, J. Jimenez-Barbero, K. K. Baldrige, A. Bernardi, *J. Am. Chem. Soc.* 2007, 129, 2890.
- [7] J. Screen, E. C. Stanca-Kaposta, D. P. Gamblin, B. Liu, N. A. Macleod, L. C. Snoek, B. G. Davis, J. P. Simons, *Angew. Chem.* 2007, 119, 3718; *Angew. Chem. Int. Ed.* 2007, 46, 3644.
- [8] R. Palma, M. E. Himmel, J. W. Brady, *J. Phys. Chem. B* 2000, 104, 7228.
- [9] a) J. C. Morales, S. PenadUs, *Angew. Chem.* 1998, 110, 673; *Angew. Chem. Int. Ed.* 1998, 37, 654; b) K. Kobayashi, Y. Asakawa, Y. Kato, Y. Aoyama, *J. Am. Chem. Soc.* 1992, 114, 10307.
- [10] a) A. P. Davis, R. S. Wareham, *Angew. Chem.* 1999, 111, 3160; *Angew. Chem. Int. Ed.* 1999, 38, 2978; b) M. Mazik, H. Cavga, P. G. Jones, *J. Am. Chem. Soc.* 2005, 127, 9045.
- [11] Y. Ferrand, M. P. Crump, A. P. Davis, *Science* 2007, 318, 619.
- [12] K. Piotukh, V. Serra, R. Borriss, A. Planas, *Biochemistry* 1999, 38, 16092.
- [13] S. E. Kiehna, Z. R. Laughrey, M. L. Waters, *Chem. Commun.* 2007, 4026.

- [14] a) M. Senior, R. A. Jones, K. J. Breslauer, *Biochemistry* 1988, 27, 3879; b) S. Bommarito, N. Peyret, J. SantaLucia, Jr., *Nucleic Acids Res.* 2000, 28, 1929.
- [15] a) E. T. Kool, J. C. Morales, K. M. Guckian, *Angew. Chem.* 2000, 112, 1046; *Angew. Chem. Int. Ed.* 2000, 39, 990; b) K. M. Guckian, B. A. Schweitzer, R. X. F. Ren, C. J. Sheils, D. C. Tahmassebi, E. T. Kool, *J. Am. Chem. Soc.* 2000, 122, 2213; c) J. C. Morales, E. T. Kool, *Biochemistry* 2000, 39, 12979.
- [16] a) U. Wichai, S. A. Woski, *Org Lett.* 1999, 1, 1173; b) S. Matsuda, F. E. Romesberg, *J. Am. Chem. Soc.* 2004, 126, 14419.
- [17] B. L. Sorg, W. E. Hull, H.-C. Kliem, W. Mier, M. Wiessler, *Carbohydr. Res.* 2005, 340, 181.
- [18] A. P. Rauter, S. Lucas, T. Almeida, D. Sacoto, V. Ribeiro, J. Justino, A. Neves, F. V. M. Silva, M. C. Oliveira, M. J. Ferreira, M.-S. Santos, E. Barbosa, *Carbohydr. Res.* 2005, 340, 191.
- [19] M. Adinolfi, L. De Napoli, G. Di Fabio, A. Iadonisi, D. Montesarchio, G. Piccialli, *Tetrahedron* 2002, 58, 6697.
- [20] a) M. Petersheim, D. H. Turner, *Biochemistry* 1983, 22, 256; b) T. Ohmichi, S. Nakano, D. Miyoshi, N. Sugimoto, *J. Am. Chem. Soc.* 2002, 124, 10367.
- [21] S. Liu, X. Ji, G. L. Gilland, W. J. Stevens, R. N. Armstrong, *J. Am. Chem. Soc.* 1993, 115, 7910.
- [22] a) L. K. Tsou, C. D. Tatko, M. L. Waters, *J. Am. Chem. Soc.* 2002, 124, 14917; b) E. Lacroix, A. R. Viguera, L. Serrano, *J. Mol. Biol.* 1998, 284, 173.

Scheme 1 **A**. Dangling-ended DNA model system designed to measure carbohydrate-aromatic interactions. **B**. Enlarged view of the structure of the dangling-end area of the carbohydrate-oligonucleotide conjugate. **C**. Carbohydrate oligonucleotide conjugates included in the study. Oligonucleotide conjugate **1** is BCGCGCG, where B is the benzene nucleoside. In conjugates **2-7**, DNA seq represents $-\text{OPO}_2^-$ -BCGCGCG.



Scheme 2. Synthetic routes used to prepare the carbohydrate phosphoramidite derivatives. (a) Ethyleneglycol, Ag_2CO_3 , CH_2Cl_2 , R.T., 18h, 28-62%; (b) 2-cyanoethyl-*N,N'*-diisopropylamino-chlorophosphoramidite, *N,N*-diisopropylethylamine (DIEA), CH_2Cl_2 , R.T., 1.5h, 74-92%; (c) ethyleneglycol, $\text{PPh}_3\cdot\text{HBr}$, CH_2Cl_2 , R.T., 7h, 5% of **23** and 20% of **24**.

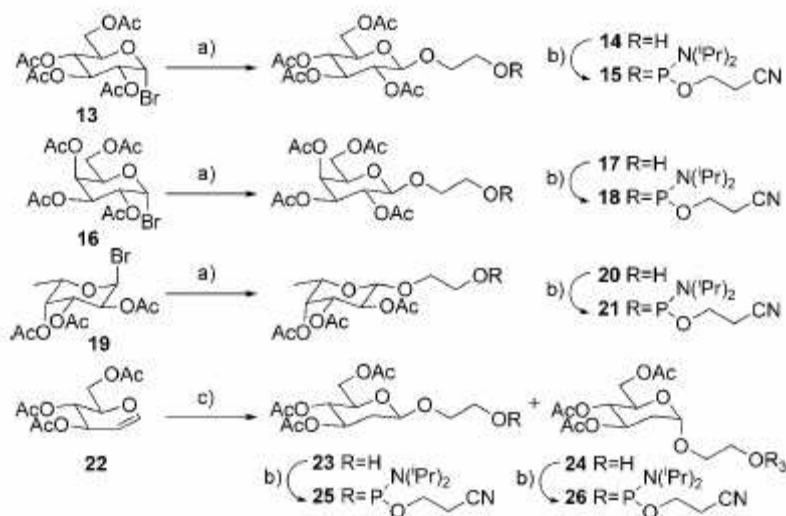


Table 1. Carbohydrate-aromatic stacking, as measured in a DNA-duplex context.

Dangling moiety ^a	<i>T</i> _m (°C) ^b	$-\Delta H^\circ$ (Kcal/mol) ^c	$-\Delta S^\circ$ (cal/K.mol) ^c	$-\Delta G_{37}^\circ$ (Kcal/mol) ^c	$\Delta\Delta G_{37}$ stacking (Kcal/mol) ^d
-	51.1	58.2	156	9.7	-
HO-C2-	50.0	56.1	150	9.4	-
β -D-Glc-C2-	51.6	63.1	171	9.9	-0.25
β -D-Gal-C2-	50.4	59.1	159	9.7	-0.15
β -L-Fuc-C2-	51.8	67.4	185	10.1	-0.40
β -D-2-deoxy-Glc-C2-	50.7	61.0	166	9.7	-0.15
α -D-2-deoxy-Glc-C2-	51.0	60.9	165	9.8	-0.20

^a Core sequence is BCGCGCG, in which B is the benzene nucleoside. C2- indicates $\text{CH}_2\text{-CH}_2\text{-OPO}_2^-$. ^b Melting temperatures, *T*_m was measured at 10 μM COC concentration. ^c Estimated errors are $\pm 8\%$ in ΔH , $\pm 8\%$ in ΔS , $\pm 11\%$ in ΔG_{37} . ^d $\Delta\Delta G_{37}$ stacking per carbohydrate-benzene pair = $(\Delta G_{\text{conjugate with carb}} - (\Delta G_{\text{conjugate with spacer}}))/2$.

Figure 1. Model of the dangling-end area of carbohydrate-DNA conjugate **4**, which contains a β -galactose unit. A) Possible stacking geometry of β -galactose on top of the benzene ring through the α face of the sugar. B) Possible stacking geometry of β -galactose on top of the benzene ring through the β face of the sugar, with the steric clash between the 4-OH group and the arene shown

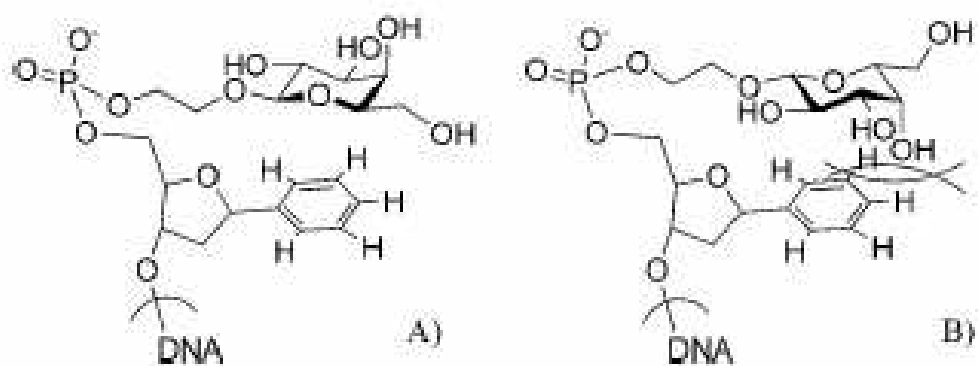


Table 2. ¹H NMR chemically induced shift differences between the sugar residues of the carbohydrate-oligonucleotide conjugates **3-7** and the corresponding monosaccharide controls **8-12** in D₂O.^[a]

	β-D-Glc	β-D-Gal	β-L-Fuc	β-D-2-deoxy-Glc	α-D-2-deoxy-Glc
H1	-0.112	-0.102	-0.144	-0.190	-0.094
H2	-0.056	-0.059	-0.084	-0.163	-0.100
H2b	-	-	-	-0.127	-0.087
H3	-0.074	-0.087	-0.082	-0.149	-0.071
H4	-0.048	-0.051	-0.093	-0.086	-0.074
H5	-0.120	-0.116	-0.178	- ^[b]	-0.067-0.067
H6	-0.069	-0.058	-	- ^[b]	- ^[b]
H6b	-0.086	-0.050	-	-0.118	-0.092
CH ₃	-	-	-0.122	-	-

^[a] Chemical-shift differences are given in ppm. ^[b] Unassigned proton due to overlapping resonances.

Figure 2. ^1H NMR spectra of carbohydrate–oligonucleotide conjugate **5** (bottom) and the corresponding monosaccharide control **10** (top) in D_2O showing the chemical-shift differences for the protons of the β -l-fucose residue

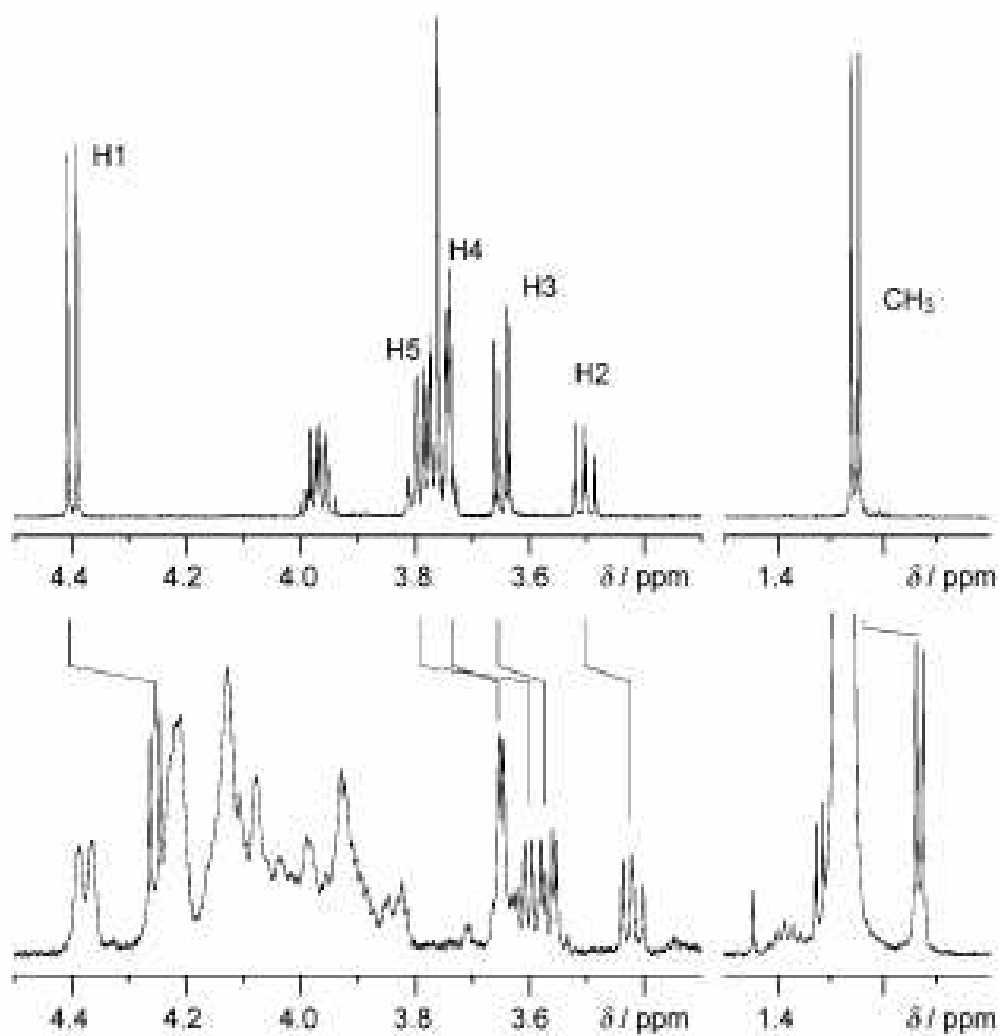


Figure 3. A) Upfield shifting of carbohydrate protons due to the proximity to the face of the aromatic ring. Differences are calculated between the conjugate containing β -D-glucose on the sequence BCGCGCG, **3**, and 2-hydroxyethyl- β -D-glucopyranoside (**8**). B) Model of possible stacking geometry of β -glucose on top of the benzene ring through the α face of the sugar. C) Model of possible stacking geometry of β -glucose on top of the benzene ring through the β face of the sugar.

